Mem. S.A.It. Vol. 77, 670

Memorie della

Cosmological evolution of galaxies and interaction-driven fueling of AGNs

N. Menci

Istituto Nazionale di Astrofisica – Osservatorio Astronomico di Roma, Via Frascati 33, I-00040 Monteporzio, Italy e-mail: menci@mporzio.astro.it

Abstract.
We discuss the role of interaction-driven starbursts and AGN feeding, and of AGN feedback in the framework of hierarchical models of galaxy formation. We review the influence of such processes on severel key properties of the galaxy and the AGN population, nemely: 1) the "downsizing" effect; 2) the bimodal color distribution of galaxies at low-intermediate redshift; 3) the observed abundance of massive, red galaxies already at redshift $z \approx 2$; 4) the evoution of the AGN luminosity functions in optical and X-rays; 5) the abundance of extremely red objects at $1.5 \leq z \leq 2.5$.

Key words. galaxies: formation — galaxies: high-redshift — cosmology: theory

1. Introduction

Linking the evolution of Active Galactic Nuclei (AGNs) to the evolution of their host galaxies into a cosmological framework constitutes a major task of "ab initio" models of galaxy formation. These envisage the build up of stars in galaxies as a gradual process driven by the continuous growth of the host dark matter (DM) galactic halos through repeated merging events. These progressively increase also the gas mass in the growing galaxies; its subsequent radiative cooling is partially counteracted by the heating due to the winds from Supernovae originated by parent massive stars. The net result of such a "quiescent" star formation is a gradual increase of the stellar content of the galaxies. The above hierachical scenario has quantitatively modeled through semi-analytic models (SAMs, Kauffman, White & Guiderdoni 1993; Cole et al. 1994; Somerville & Primack & Faber 2001; Cole et al. 2000, Menci et al. 2002) which connect the star formation rate to the gas cooling processes through phenomenological scaling laws.

In such a context, the growth of Supermassive Black Holes (SMBHs) has been connected to the cold gas available in the host galaxy to the BH accretion (powering AGNs) either assuming phenomenological and tunable scaling laws (e.g., Kauffmann & Haehnelt, 2000) or assuming major galaxy mergers at high z as the only triggers for BH accretion (see, e.g., Haiman & Loeb 1998; Wyithe & Loeb 2002; Volonteri, Hardt & Madau 2003).

Although the above models succeded in matching several observables concerning the global behaviour of galaxy evolution, like the evolution of the density of star formation (and UV emission) from $z = 0$ to $z = 4$, and the

Send offprint requests to: N. Menci

QSO density at $z \geq 1.5$, they compare critically with several recent observations. In particular:
1) the predicted amount of stars formed at high z in the *bright* galaxy population is lower than indicated by several observational results. In fact, SAMs underpredict both the bright end of the K-band luminosity functions at intermediate redshifts ($z \approx 1-2$, see Pozzetti et al. 2003) and the abundance of galaxies brighter than $K = 20$ at $z > 1.5$ (Cimatti et al. 2002). The above observations imply that the star content of massive galaxies already in place at $z \approx 2$ is larger than that resulting from the gradual star formation typical of hierarchical models. Indeed, independent, direct observations at $z \approx 2$ of the stellar mass density of massive galaxies (in the range $m_* \approx 10^{10}-10^{11}$ $M_\odot$) yield a fraction close to 0.3 of the present value, while the canonical SAMs yield a fraction around 0.1 (see Fontana et al. 2003).
2) the strong observed "downsizing" (i.e., older stellar populations in the most massive galaxies) is only mildly reproduced in the model; also, observations indicate the existance of a bimodal partition in the color distribution of galaxies (Strateva et al. 2001; Baldry et al. 2004) extending at least up to $z \approx 1.5$ (Bell et al. 2004, Giallongo et al. 2005), which defines two classes of galaxies; a red population, consisting mostly of galaxies which have formed most of their stellar mass at high redshifts z, and a blue population consisting of galaxies actively forming stars. The fraction of galaxies belonging to the red population grows with the luminosity L, being smaller than the blue fraction for $M_r > -19.5$ and dominating the distribution for $M_r < -21$. The models fail to reproduce the correct fraction of red/blue objects, both locally and (more severly) at high redshift $z \approx 1.5-2.5$, when the abundance of extremely red objects (EROs, with optical infra-red colors redder than a passively evolving elliptical, $R - K > 5$) is underestimated by present hierarchical models (see McCarthy et al 2004; Cimatti et al. 2004; Daddi et al. 2005; Somerville et al. 2004) by factors of order ten (depending on the exact color and magnitude cut).
3) On the AGN side, the canonical models fail to reproduce the observed dramatic drop of the quasar (QSOs) and X-ray emitting AGNs population between $z \approx 1.5$ and the present, indicated by, e.g., the decline of ≈ 3 dex of the number density of bright ($M_B < -26$) QSO from $z = 2$ to the present (see, e.g., Hartwick & Shade 1990).

To address the above points, we have built up a SAM which includes the growth of SMBHs and the ensuing AGN activity by assuming the galaxy interactions (merging and fly-by) as the trigger for BH accretion and for starbursts (Menci et al. 2003, 2004, 2005). Such interactions mainly involve massive galaxies (characterized by larger cross section for interactions) at high redshift (where the space density and of galaxy was much larger than the present), thus providing, at the same time, an increase in the amount of stars formed at high redshift in massive galaxies and, due to the strong decline of the interaction rate at $z \leq 2.5$, a rapid decline of the bright quasar population. The model also includes the feedback of AGNs on the star formation of the host galaxy due to the energy injected by the AGN emission on the interstellar gas (Menci et al. 2006).

Here we review how the model including the galaxy interactions and the AGN feedback may provide a unified framework to naturally fit the points 1)-3) mentioned above.

2. The model of Galaxy formation

We adopt the SAM described in Menci et al. (2005); this connects the baryonic processes (gas cooling, star formation, Supernovae feedback) to the merging histories of the DM haloes (with mass M, virial radius R and mass m) and of the galactic sub-haloes (with mass m, tidal radius r_t and circular velocity v) following the canonical recipes adopted by SAMs of galaxy formation. The merging histories of the host haloes, and the dynamical friction and binary aggregations acting on the included sub-halos, are computed adopting the canonical Monte Carlo technique as in Menci et al. (2005).

The properties of the baryons (gas and stars) contained in the galactic DM clumps are computed as follows. Starting from an initial amount $m\,\Omega_b/\Omega$ of gas at the virial temperature of the galactic halos, we compute the mass m_c of cold baryons within the cooling radius. The disk associated to the cold baryons will have a radius r_d, rotation velocity v_d, and dynamical time $t_d = r_d/v_d$, all computed after Mo, Mao & White (1998). As for the star formation, we assume the canonical Schmidt form $\dot{m}_* = m_c/(q\,\tau_d)$, where $\tau_d \equiv r_d/v_d$ and q is left as a free parameter. At each time step, the mass Δm_h returned from the cold gas to the hot gas phase due to Supernovae (SNe) activity is estimated from canonical energy balance arguments (see, e.g., Kauffmann & Charlot 1998) as $\Delta m_h = E_{SN}\,\epsilon_0\,\eta_0\,\Delta m_*/v^2$ where Δm_* is the mass of stars formed in the timestep, $\eta \approx 3-5\cdot 10^{-3}/M_\odot$ is the number of SNe per unit solar mass (depending on the assumed IMF), $E_{SN} = 10^{51}$ ergs is the energy of ejecta of each SN; $\epsilon_0 = 0.01-0.5$ is the efficiency of the energy transfer to the cold interstellar gas. The model free parameters $q = 30$ and $\epsilon_0 = 0.1$ are chosen as to match the local B-band LF and the Tully-Fisher relation adopting a Salpeter IMF.

In the following, we shall assume the following set of cosmological parameters: $\Omega_0 = 0.3$, $\Omega_\Lambda = 0.7$, $\Omega_b = 0.05$ and $H_0 = 70\,\mathrm{km\,s^{-1}\,Mpc^{-1}}$; the metallicity and the dust extinction are computed as in Menci et al. (2002), as well as the evolution of the stellar populations, with emission derived from synthetic spectral energy distributions (Bruzual & Charlot 1993), adopting a Salpeter IMF.

The consistency of our set of cooling, star formation and feedback laws with the available observations has been checked in Menci et al. (2005) by comparing with the local observed distribution of cold gas, stars and disk sizes, with the Tully-Fisher relation in the I-band. We compared also with the B-band (at low z) and the UV (at high z) luminosity functions, to show that the instantaneous star formation implemented in the model is consistent with observations over a wide range of cosmic times.

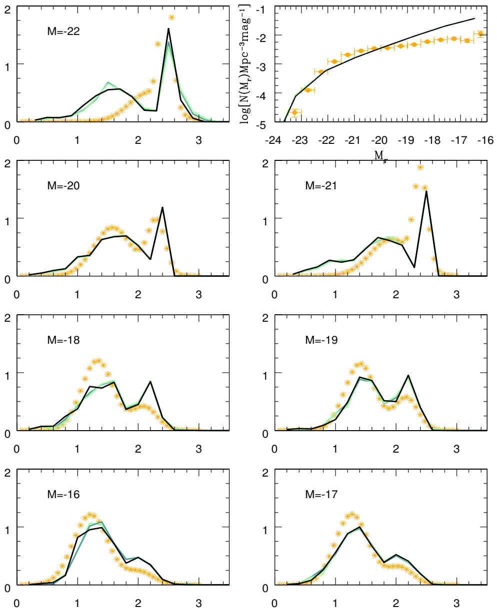

Fig. 1. The predicted rest-frame $u-r$ color distributions (heavy lines) are compared with the SDSS data (Baldry et al. 2004, stars) for different magnitude bins. The distributions are normalized to the total number of galaxies in the magnitude bin; the normalization of the data and of the model predictions are given by the r-band LFs shown in the top-right panel.

2.1. The Downsizing in Hierarchical Clustering Scenario

We compare in fig. 1 the color distribution resulting from our model for different luminosity bins with the Gaussian fit to the observational points from the Sloan survey (SDSS), given in Baldry et al. (2004) for the $u-r$ colors; details on the SDSS u and r bands are given by the above authors.

Note that: 1) the most massive galaxies have redder colors and older stellar populations (downsizing); 2) there is a sharp partition between red and blue galaxies. Hierarchical clustering provides a framework for the rising of bimodality because of two natural features: i) star formation histories of massive galaxies and of galaxies formed in biased, high density regions are peaked (on average) at higher z compared to lower mass galaxies; ii) the existence of a non- gravitational mass scale m_0 (corresponding to $v \approx 100$ km/s) such that for $m < m_0$ the star formation is self-regulated and the cold gas content is continuously depleted by effective feedback.

In fact, merging histories leading to the local red population are characterized by a progenitor distribution skewed toward masses larger than m_o at high $z \approx 4-5$. In such progenitors, feedback is ineffective in reheating/expelling the cold gas content and, if the latter is rapidly converted into stars at $z \approx 4-5$, the main progenitors exhaust their cold gas reservoir at $z \approx 2$ and thereafter undergo an almost quiescent phase characterized by a fast drop of $\dot{m}_*$. Massive galaxies and galaxies formed in a biased region of the primordial density field (which later become the galaxy environment) are preferentially assembled through the former kind of merging history. Merging histories leading to the local blue population are characterized by a progenitor distribution dominated by small- mass progenitors. There the star formation is self-regulated by feedback (effective in reheating/expelling gas in galaxies with mass $< m_0$), which limits the cold gas content and is effective in prolonging the active phase of star formation. Small-mass galaxies are generally built-up through this evolutionary path.

2.2. Interactions Triggering Starbursts

The inclusion of starbursts in the hierarchical models of galaxy formation enhances the early star formation in the progenitors of massive galaxies.

In our model, interactions (both fly-by and merging) destabilize part of the galactic cold gas due to the induced loss of orbital angular momentum. The rate of interactions is

$$\tau_r^{-1} = n_T\, \Sigma(v, V)\, V_{rel}. \qquad (1)$$

Here n_T is the number density of galaxies in the same halo, V_{rel} is their relative velocity, and the cross section $\Sigma \approx \pi(r_t^2 + r_t^{'2})\,[1 + (v/V_{rel})^2]$ is averaged over all partners with tidal radius r_t'.

The fraction of cold gas funnelled toward the centre is computed in terms the variation Δj of the specific angular momentum $j \approx Gm/v_d$ of the gas, to read (Cavaliere & Vittorini 2000; Menci et al. 2003)

$$f_{acc} \approx \frac{1}{2}\left|\frac{\Delta j}{j}\right| = \frac{1}{8}\left\langle \frac{m'}{m}\,\frac{r_d}{b}\,\frac{v_d}{V_{rel}}\right\rangle. \qquad (2)$$

Here b is the impact parameter, evaluated as the average distance of the galaxies in the halo. Also, m' is the mass of the partner galaxy in the interaction, and the average runs over the probability of finding such a galaxy in the same halo where the galaxy m is located. We assume that $3/4$ of the destabilized gas $f_{acc}\, m_c$ is converted into starbursts (see Sanders & Mirabel 1996), while the rest feeds BH accretion (see below).

Note that both the interaction rate τ_r^{-1} and the accreted fraction f_{acc} decrease with increasing cosmic time t, due to the lower cross section of galaxies in environments with growing size, and to their increasing relative velocities, so that starbursts are expected to take place mainly at $z \geq 2.5-3$.

In fig. 2 we compare the results with observations obtained from the K20 survey (Cimatti et al. 2002; Pozzetti et al. 2003). The starbursts brighten the LF by ~ 0.5 mag at $z \approx 1.5$, so matching the observed shape of the LFs (top panel). Meanwhile the faint end of the LFs is left almost unchanged. This is a consequence of the larger effectiveness of the bursts in more massive galaxies, which is due to the physics of interaction-driven bursts combining with the statistics of encounters. On the one hand, in each bursts galaxies with larger disk sizes undergo larger losses of angular momentum as a consequence of larger gravitational torques; on the other hand, larger galactic sizes favor the encounters. Correspondingly, the burst model *matches* the observed number of luminous ($m_K < 20$) galaxies at $z \geq 1.5$, while the quiescent model underpredicts the number by a factor $\sim 3-4$ (see bottom panel in fig. 2).

3. The Evolution of AGNs

The feeding of SMBHs and the corresponding AGN phase naturally fits in the above model of galaxy evolution. In fact, a fraction q_{acc} of the gas destabilized by the galaxy interactions is

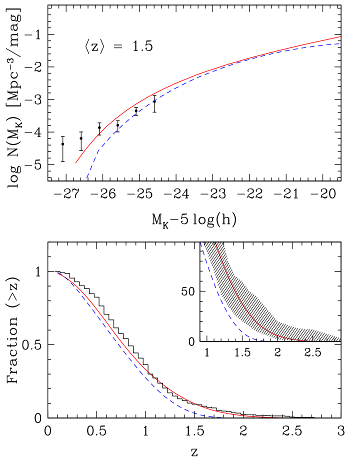

Fig. 2. Upper panel: the K-band galaxy LFs at $z = 1.5$ in the quiescent (blue dashed line) and in the starburst model (red solid line) are compared with the data from the K20 survey (Pozzetti et al. 2003). Bottom panel: the corresponding cumulative z-distribution of $m_K < 20$ galaxies are compared with observations from the K20 survey (Cimatti et al. 2002). The inset shows in detail the cumulative distribution in the range $1 < z < 3$ with the 3σ Poissonian confidence region (shaded area).

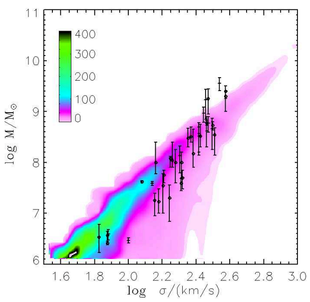

Fig. 3. The derived relation between the BH mass and the 1-D velocity dispersion of the host galaxy (solid line) is compared with data from Ferrarese & Merritt (2000, filled squares) and Gebhardt et al. (2000, circles).

funneled toward the central SMBH: the resulting accreted mass $\Delta m_{acc} = q_{acc}\, f_{acc}\, m_c$ powers the AGN emission with bolometric luminosity

$$L(\nu, t) = \frac{\eta\, c^2 \Delta m_{acc}}{\tau}\ . \qquad (3)$$

We set $q_{acc} = 1/4$ (see below eq. 2) and the duration of an accretion episode, i.e., the timescale for the QSO to shine, is assumed to be the crossing time for the destabilized cold gas component, $\tau = r_d/v_d$; the energy-conversion efficiency is taken $\eta = 0.1$ (see, e.g., Yu & Tremaine 2002). The SMBH mass m_{BH} grows through the accretion described below and by merging with other SMBH during galaxy merging, assuming in all galaxies small seed BHs of mass $10^2\, M_\odot$ (Madau & Rees 2001).

In our Monte Carlo model, at each time step we assign to each galaxy an active BH accretion phase (with duration τ) with a probability given by eq. (1). In such a phase, we compute the accreted cold gas and associated QSO emission through equations (2) and (3). In fig. 3 we test the consistency of the host galaxy-SBMH connection resulting from our model by comparing with the observed correlation between the local BH mass m_{BH} and the 1-dimensional velocity dispersion of stars in the host galaxy.

The evolution of the QSO luminosity function is shown in fig. 4. Note the strong evolution from $z \approx 0.5$ to $z \approx 2$, due to 1) the declining $\Delta m_{acc}(z)$ 2) the timescale τ shortening at higher z; 3) the exhaustion of the cold gas reservoir already converted into stars at larger z; 4) the declining galaxy merging and interaction rate.

4. The Feedback from AGNs onto the Host Galaxies

Despite their success in reproducing the bimodal feature of the local color distributions, when one focuses on the observed proportion of red/blue galaxies it is found that current hierarchical models underestimate the number of luminous/massive *red* galaxies (see, e.g., fig. 1 top-left panel), in particular at high redshift $z \approx 1.5 - 2.5$ when the abundance of extremely red objects (EROs, with optical infra-red colors redder than a passively evolving elliptical, $R - K > 5$) is underestimated by present hierarchical models (see, e.g, Somerville et al. 2004) by factors of order ten (depending on the exact color and magnitude cut).

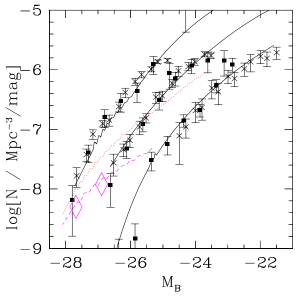

Fig. 4. The QSO luminosity functions in the B-band (obtained applying a bolometric correction of 13 to the luminosity in eq. 3) from our model (solid lines) are shown for $z = 0.55$, $z = 1.2$, and $z = 2.2$ (lower, middle and uppermost curve, respectively). The data points are taken from Hartwick & Shade (1990, solid squares) and Boyle et al. (2000, crosses), and rescaled to our cosmology. The dashed and dotted lines are the model prediction for $z = 4.2$ (compared to the Sloan data from Fan et al. 2001, diamonds) and $z = 3.4$, respectivley

Here we investigate the effect of the energy injection from the AGNs onto the interstellar gas of the host galaxy. The relevance of such a process on the galaxy evolution is receiving increasing observational support from the observations of massive outflows of ionized gas from the galactic nuclei, characterized by high-velocities (up to 0.4 c) indicating mass flows of 1-10 $M_{\odot}$/yr (see Chartas 2002; Crenshaw, Kramer, George 2003; Pounds et al. 2003), and from aimed numerical simulations of colliding galaxies (Di Matteo et al. 2005).

We adopt for such a feedback the model by Cavaliere, Lapi & Menci (2002). They investigated the blowout of interstellar gas due to energy injection ΔE by AGNs by computing the propagation of the shockwave in the interstelar gas (including the effects of gravity and of the gas density gradient). After the passage of the blast-wave the gas left over recovers hydrostatic equilibrium to a new temperature lower than the initial by a factor β. The values of Δm and β for any given ratio $\Delta E/E$ are tabulated in Cavaliere, Lapi & Menci (2002). In our semi-analytic model, for any galaxy undergoing an active AGN phase (see sec. 2.1), we compute $\Delta E = f\,L\,\tau$ (and the corresponding effect on Δm and β) assuming the AGN feedback efficiency $f = 5\,10^{-2}$.

The energy injection from AGNs on the color distribution of local galaxies affects primarely the color distribution of very luminous ($M_r < -22$) galaxies. due to their larger cross section for interactions (triggering the AGN activity) and to the larger fraction of destabilized gas accreted by the SMBH (powering the AGN activity). Note how the inclusion of AGN feedback makes the color distribution of such objects entirely dominated by red objects (left panel of fig. 5). We expect the effect of the AGN feedback directly related to the bright QSO phase to become more important with increasing z, due to the enhanced AGN activity at such cosmic epochs. In particular, we expect that the inclusion of the AGN feedback will solve the long-standing problem of semi-analytic models related to their severe underestimate of EROs. Such a point is addressed in the right panel of fig. 5, where we plot the observed-frame $R - K$ color distribution of $K < 20$ (Vega system) galaxies in the redshift range $1.7 < z < 2.5$ and compare it with the observed distribution. Note how the inclusion of AGN feedback strongly enhances the number of predicted EROs with respect to the no-AGN feedback case.

5. Conclusions

The model presented here connects into a single framework several relevant aspects of the evolution of galaxies and AGNs. In particular:

1) The destabilization of galactic gas triggered by galaxy interaction, causing both starbursts and AGN activity mainly in the progenitors of massive galaxies at $z \geq 2.5-3$, naturally provides

• early assembly of stellar mass in the progenitors of local, massive ($M_* \geq 5\,10^{10}\,M_{\odot}$) galaxies; the resulting stellar mass distribution and the related K-band luminosiyt functions and counts agree with observations up to $z \approx 2$.

• rapid drop of the number density of bright QSO from $z \approx 2.5$ to the present; the corresponding QSO luminosity functions match the observations from $z = 4$ to the present.

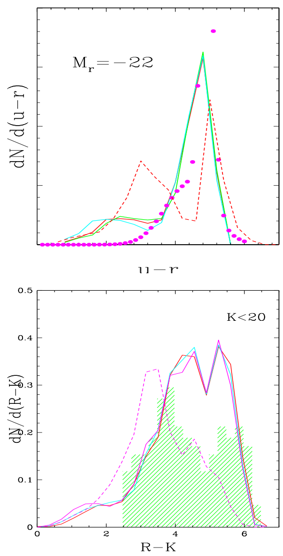

Fig. 5. Left panel: the local $u - r$ color distribution of $M_r \leq -22$ galaxies resulting from the model including AGN feedback (solid line) is compared with the previous case (no AGN feedback, (dashed line). Data as in fig. 1. Right panel: The observed frame $R - K$ color distribution from the GOODS data (histogram) are compared with the results of the model with no AGN feedback (dashed line) and of the model including the AGN feedback (solid line).

2) The conversion of galactic gas into stars is larger in the progenitors of massive galaxies. In our model, this results into

• Downsizing: while hierarchical models predict massive objects to be assembled at later cosmic times, they also predict their progenitor clumps to be formed in biased-high density regions of the primordial density field, where the enhanced density allowed early star formation, and galaxy interactions are more effective in triggering starbursts. Note that the same argument applies to the accretion history of SMBHs, so that a downsizing scenario is naturally predicted also for AGNs (see Menci et al. 2004b).

• Bimodal color distribution. The model naturally provides a non- gravitational mass scale m_0 (corresponding to $v \approx 100$ km/s) such that for $m < m_0$ the star formation is self-regulated and the cold gas content is continuously depleted by effective feedback. In the shallow potential wells of the progenitors of local faint galaxies, this results into a smooth star formation history, and the star formation is prolonged down to $z = 0$. In the deepest potential wells of the progenitors of local, massive galaxies, the early star formation results into an exhaustion of cold gas reservoir at $z \approx 2$, and the galaxies undergo a passive evolution (with only occasional episodes of star formation) from $z \approx 2$ to the present. 3) The effect of AGN feedback onto the star formation history of galaxies. The bimodal color distribution is not determined by the AGN feedback, as we showed in Menci et al. (2006) and as confirmed by the recent results by Croton et al.(2006); rather, AGN feedback affects the partition of galaxies between the blue and the red population, enhancing the fraction of red galaxies. In particular

• The distribution of local very luminous ($M_r < -22$) galaxies is dominated by red objects when AGN feedback is included, in agreement with observations.

• The bimodal behaviour of the color distribution is extended to $z \approx 3$. AGN feedback is effective in suppressing the star formation of massive galaxies at $1.5 \leq z \leq 2.5$; this enhaces the predicted fraction of galaxies with red colors in such a redshift range, as to match th observed abundance of EROs.

References

Baldry, I.K. et al. 2004, ApJ, 600, 681
Bell, E., et al. 2004, ApJ, 608, 752
Boyle, B.J. et al. 2000, MNRAS, 317, 1014
Bruzual, A.G., & Charlot, S., 1993, ApJ, 105, 538
Cavaliere, A., Vittorini, V., 2000, ApJ, 543, 599
Cavaliere, A., Lapi, A., Menci, N., 2002, ApJ, 581, L1
Cimatti, A. et al. 2002, A&A, 392, 395
Cimatti, A. et al. 2004, Nature, 430, 184
Chartas, G., Brandt, W. N., Gallagher, S. C., Garmire, G. P., 2002, ApJ, 579, 169
Cole, S., et al. 1994, MNRAS, 271, 781
Cole, S., et al. 2000, MNRAS, 319, 168
Crenshaw, D.M., Kraemer, S.B.. George, I.M. 2003, ARA&A, 41, 11
Croton, D.J. et al. 2006, MNRAS, 365, 11

Daddi, E. et al. 2005, ApJ, 626, 680
Di Matteo, T., Springel, V., Hernquist, L., 2005, Nature, 433, 604
Fan, X. et al., 2001, ApJ, 121, 54
Ferrarese, L. Merritt, D., 2000, ApJ, 539, L9
Fontana, A. et al. 2003, ApJ, 594, L9
Gebhardt, K. et al., 2000, ApJ, 539, L13
Giallongo, E. et al. 2005, ApJ, 622, 116
Haiman. Z., & Loeb, A., 1998, ApJ, 503, 505
Hartwick, F.D.A., Shade, D., 1990, ARA&A, 28, 437
Kauffmann, G., White, S.D.M., & Guiderdoni, B., 1993, MNRAS, 264, 201
Kauffmann, G., Charlot, S. 1998, MNRAS, 294, 705
Kauffmann, G., Haehnelt, M., 2000, MNRAS, 311, 576
Madau, P., & Rees, M.J., 2000, ApJ, 551, L27
McCarthy, P.J. 2004, ARA&A, 42, 477
Menci, N., et al. 2002, ApJ, 578, 18
Menci, N., et al. 2003, ApJ, 587, L63
Menci, N., et al. 2004b, ApJ, 606, 58
Menci, N., et al. 2005, ApJ, 632, 49
Menci, N., et al. 2004, ApJ, 604, 12
Menci, N., et al. 2006, submitted
Mo, H.J, Mao S., & White, S.D.M., 1998, MNRAS, 295, 319
Pozzetti, L. et al. 2003, A&A, 402, 837
Pounds, K., et al. 2003, MNRAS, 346, 1025
Sanders, D.B., & Mirabel, I.F. 1996, ARA&A, 34, 749
Schneider, S.E., 1997, PASA, 14, 99
Somerville, R.S., Primack, J.R., & Faber, S.M., 2001, MNRAS, 320, 504
Somerville, R.S., et al. 2004, ApJ, 600, L135
Strateva, I. et al. 2001, AJ, 122, 1861
Volonteri, M., Haardt, F., Madau, P., 2003, ApJ, 582, 559
Wyithe, J.S., Loeb, A. 2002, ApJ, 581, 886
Yu, Q., & Tremaine, S., 2002, MNRAS, 335, 965